Journal of Russian Laser Research, Volume 31, Number 5, 2010

TRANSFER OF MICROWAVE RADIATION IN SLIDING MODES OF PLASMA WAVEGUIDES

Igor V. Smetanin,[1*] Vladimir D. Zvorykin,[1,2] Alexey O. Levchenko,[1,2] and Nikolay N. Ustinovsky[1,2]

[1] *P. N. Lebedev Physical Institute, Russian Academy of Sciences Leninskii Prospect 53, Moscow 119991, Russia*

[2] *Advanced Energy Technologies Ltd., Neglinnaya Street 14, Moscow 107031, Russia*

*Corresponding author e-mail: smetanin @ sci.lebedev.ru

Abstract

We study experimentally and theoretically a new regime of the sliding-mode propagation of microwave radiation in plasma waveguides in atmospheric air. We show that a plasma waveguide of large radius (much larger than the wavelength of the signal) can be developed in the photoionization of air molecules by the KrF-laser emission. We demonstrate the transfer of a 38 GHz microwave signal to a distance of up to 60 m. The mechanism of the transfer is determined by total internal reflection of the signal on the optically less dense walls of the waveguide. We perform the calculations for waveguides of various radii and microwave radiation wavelengths and show that the propagation increases with decrease of the wavelengths and reaches several kilometers for submillimeter waves.

Keywords: plasma waveguide, sliding mode, KrF laser, photoionized plasma, plasma filaments.

1. Introduction

The properties of plasma waveguides have been studied in a large number of works during the recent decades because this problem is closely related to issues of acceleration of charged particles in plasma, amplification and generation of microwave radiation, its transfer, microwave heating, and diagnostics of plasma, diffraction on plasma formation, and a range of other problems [1]. Transfer of electromagnetic (microwave and radiofrequency) radiation pulses in atmospheric air using the laser plasma as a guiding structure has been proposed in [2,3], and the waveguide properties of the laser spark have been experimentally demonstrated in [4–6].

The development of plasma structures up to several tens and hundreds of meters long became possible with the discovery of the effect of filamentation of high-power ultrashort laser pulses [7–9]. In the process of filamentation, when a laser pulse propagates in atmospheric-pressure gases, a trace is formed in the shape of a thin plasma filament $\leq$100 μm in diameter, electron density $10^{15} - 10^{17}$ cm^{-3}, and several hundred meters long. From the viewpoint of a number of applications, it appears interesting to use such plasma formations controlled by their geometry and characteristics (density profile, etc.) for tasks involving electromagnetic-radiation transfer. The propagation of 3D modes of microwave radiation in hollow plasma waveguides, whose walls are formed by these filaments, was theoretically investigated

Translated from a manuscript submitted on August 7, 2010.

1071-2836/10/3105-0495

in [10]. The optimum choice of the plasma waveguide radius was found to be of the order of the wavelength of the signal, $R \sim \lambda$.

The transfer regime is provided by the high conductance of the plasma in the channel; thus, the physical mechanism is quite similar to the traditional case of waveguides with metal walls. The conductance of plasma, however, is several orders of magnitude lower than that of metal and, as a result, the signal propagates only to an insignificant distance. In [11] the experiment was performed in a waveguide ∼4.5 cm in diameter, formed by multiple filaments, to demonstrate the transfer of a 10 GHz microwave signal to a distance of ∼16 cm. Numerical calculations show [12] that some increase in the transfer length can be achieved in structures formed by orderly arranged plasma filaments of the type of photonic crystals.

In this work, we investigate experimentally and theoretically an alternative mechanism of the sliding-mode propagation of microwave radiation inside a hollow plasma channel of large radius $R \gg \lambda$, which makes it possible to increase significantly the signal transfer length. Such a possibility with the use of a tubular UV laser beam was first indicated in [3], and its realization using a KrF laser was reported in [13]. Physically, this mechanism is based on the effect of total reflection at the interface with an optically less dense medium. For waveguides of a sufficiently large radius, lower modes become "sliding" — the transverse wavenumber is significantly ($\sim\lambda/R$ times) smaller than the longitudinal wavenumber, and the effective angle of incidence on the reflection surface exceeds the critical angle determined by the ratio of the refractive indices of air and plasma. With this approach, high conductance of the plasma is not required, which makes it possible to be restricted to a low degree of air ionization, with plasma density of 10^{11}–10^{14} cm^{-3}.

We should emphasize the difference between plasma waveguides used in our work and large-radius dielectric waveguides [14, 15]. Those waveguides are, in particular, capillary tubes with dielectric walls; high-power laser radiation propagating in the waveguides ionizes the gas filling the capillary tube and forming the plasma wave for acceleration of electrons [16–18]. The mode analysis in such a structure is presented in [15]. In such dielectric waveguides, reflection occurs at the boundary of the wall with larger permittivity than inside the capillary, and the losses emerge owing to the leakage of radiation through the capillary wall. In contrast, in plasma waveguides, there exists total internal reflection from the optically less dense walls, and the modes are attenuated owing to the conductance of the plasma.

In this paper, we develop the approach of [19, 20] and give a detailed description of the experiments on efficient channeling and transfer of the sliding mode of a microwave signal in large-radius plasma waveguides formed as a result of the photoionization of atmospheric air molecules in the field of a KrF excimer laser (Sec. 2). In Sec. 3, we study the propagation of the sliding modes in plasma waveguides and present the results of numerical and analytical investigation of the roots of the dispersion equations describing the propagation of the lowest sliding axial-symmetric modes E_{01} and H_{01} of a plasma cylindrical waveguide (Sec. 3.2), as well as of the hybrid mode EH_{11} (Sec. 3.3). Finally, in Sec. 3.4 we investigate the effect of wall thickness of plasma waveguides on the attenuation increment by the example of the axial-symmetric mode E_{01}, for which we deduce and numerically investigate the corresponding dispersion relation where the wall thickness is taken into account.

2. Experimental Realization of Sliding Modes in Plasma Waveguides

Below, we present the results of the first experiments on the efficient channeling and transfer of the sliding mode of a microwave signal in a plasma waveguide of a comparatively large radius $R \approx 5$ cm

formed in atmospheric air by the radiation of a GARPUN KrF excimer laser [21]. In the unstable-resonator injection control regime, the laser generated pulses of ∼70 ns at the half-height, an energy of ∼50 J, and radiation divergence $\sim 10^{-4}$ rad. To obtain a parallel, convergent or divergent "tubular" beam, we used various optical setups (Fig. 1).

In setup (a), the central part 100–120 mm in diameter was shut in the initial laser beam 180×160 mm in transverse size by means of a round closure. Herewith, the average radiation intensity (in the beam cross section) did not exceed $I = 2 \cdot 10^6$ W/cm^2, and the photoelectron density in air was, according to the plasma conductance measurements [19], $n_e \sim 2 \cdot 10^8$ cm^{-3}. To increase the electron density by three orders of magnitude, readily ionized hydrocarbon vapors were added to atmospheric air.

In setup (b), the initial beam was compressed by a two-lens telescope (Fig. 2a) and, with the use of two axicons (conical lenses), was transformed without energy losses into a tubular beam 120 mm in outer diameter and 10 mm "wall" thickness (Fig. 2b). The minor part of energy (in experiments on the propagation of microwave radiation it was blocked by the emitter) was concentrated in the center due to the parasitic reflection from the optical surfaces without antireflection coating. In this setup, the average radiation intensity in the ring was $I = 10^7$ W/cm^2, the electron density increased in air up to $n_e \sim$

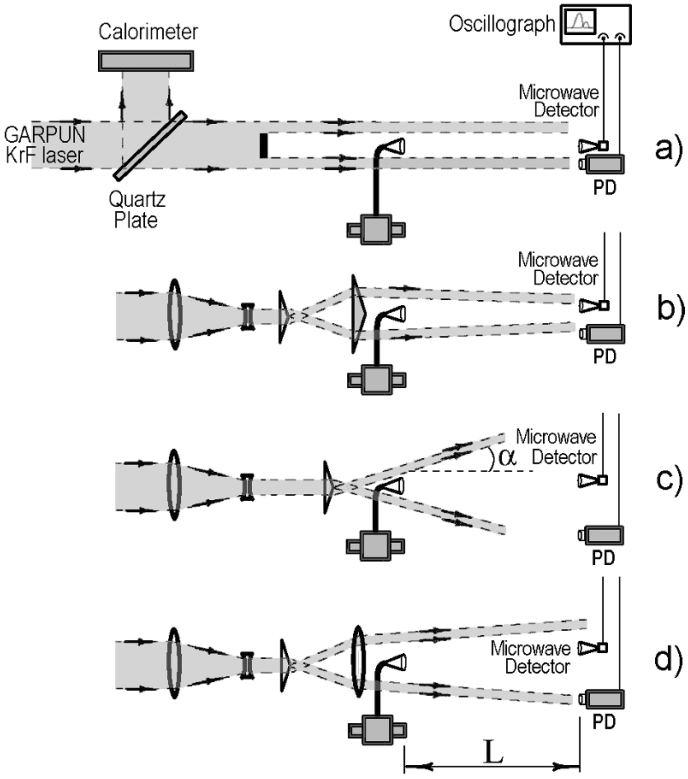

Fig. 1. Various setups of experiments on the microwave radiation propagation in plasma waveguides.

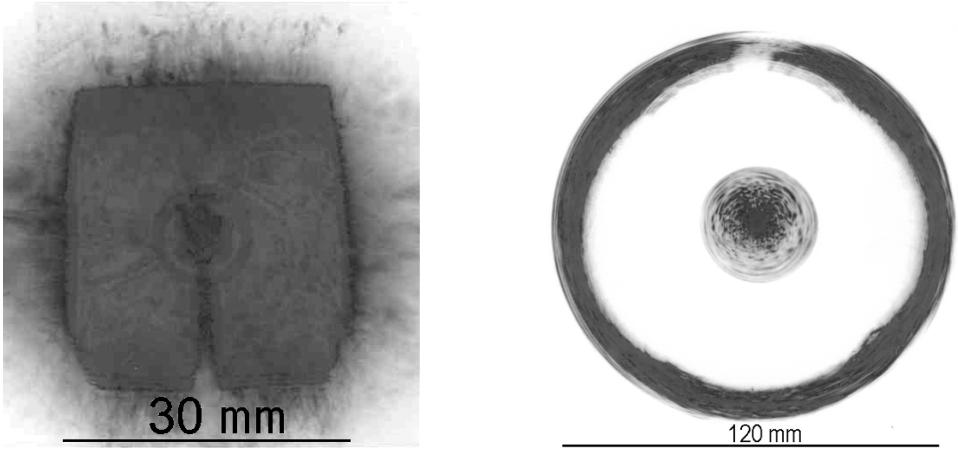

Fig. 2. Laser-beam prints on a photo paper after a two-lens telescope (left) and a two-axicon telescope (right).

10^9 cm^{-3} and, correspondingly, upon the addition of hydrocarbons, up to $n_e \sim 10^{12}$ cm^{-3}. Due to a small difference in the refractive angles, the tubular beam in these experiments was convergent: its diameter decreased two times at a distance of about 15 m along the axis.

In setup (c), we used one axicon, and the tubular beam converged with an angle of 2.4°.

In setup (d), use was made of a combination of an axicon and a lens, which decreased the convergence angle of the tubular beam down to ∼1°.

As a source of microwave radiation, we used a pulsed magnetron with a peak output power of 20 W at a frequency of 35.3 GHz (wavelength, 8.5 mm). The microwave source, equipped with a conical horn transmitter antenna 25 mm in diameter, had a total angle of radiation convergence of about 30°. The microwave radiation receiver with the same horn was positioned at various distances L from the emitter. In pure air, no noticeable change of the microwave signal was observed in the presence of a tubular laser beam in either of the schemes studied. The reason for this was the insufficient photoelectron density responsible for the formation of a virtual plasma waveguide. Upon addition of hydrocarbon vapors along the propagation route, we observed the interaction of the microwave radiation with the photoionized plasma of the waveguide. Characteristic signals from the receiver and a synchronized laser pulse are shown in Fig. 3. The oscillograms on the left-hand side correspond to the case where the laser beam was closed by the screen.

Depending on the scheme of the experiments and the laser radiation intensity (respectively, the electron density in the waveguide wall), we observed that during the laser pulse the microwave signal either was absorbed in setup (a) (see Fig. 3a) or increased in setups (c) and (d) (see Fig. 3b). The largest increase in the microwave-signal amplitude, up to 6 times, was observed in setup (d) at a distance $L = 60$ m from the laser to the receiver. In setup (b) where the tubular laser beam converged, the microwave signal almost did not change.

The mechanism of microwave radiation channeling in a weakly ionized plasma waveguide is related to the reflection of radiation from the electron-density gradient at the plasma–air interface. This effect is similar to total internal reflection of optical radiation in optical fibers, but differs by the occurrence of microwave radiation in the waveguide plasma. The sign of the effect (amplification or absorption of microwave radiation) is determined by the balance of these two factors. Thus, absorption predominates at low laser intensities and electron densities in setup (a). At higher laser intensities in setups (c) and (d), the microwave radiation is amplified due to its channeling.

A qualitative condition for the microwave-radiation channeling in a geometric approximation (strictly speaking, true when the waveguide diameter $D \gg \lambda_{\text{microwave}}$) is the condition that the diffraction angle of convergence of microwave radiation $\beta_{\text{microwave}} \approx \lambda_{\text{microwave}}/D$ is smaller than the angle of total internal reflection Θ determined by the relation $\cos\Theta = n$, where n is the refractive index of ionized gas with respect to air (Fig. 4a). For small sliding angles, the expression for Θ is transformed to the form $\Theta^2 \approx \Omega_p^2/(\omega^2 + \nu_T^2)$, where $\Omega_p = \sqrt{4\pi n_e e^2/m_e}$ is the plasma frequency and ν_T is the characteristic transfer frequency of electron collisions.

Figure 5 presents the values of the diffraction angle and total internal reflection angles for pure air and volatile hydrocarbon vapors versus the microwave radiation wavelength. It is seen that for $\lambda = 8$ mm (shown by the vertical line) $\beta_{\text{microwave}} > \Theta$, and radiation channeling is impossible. With the addition of a hydrocarbon, the diffraction angle $\beta_{\text{microwave}}$ is already slightly larger than the angle of total internal reflection Θ. Owing to this, the microwave radiation channeling in a convergent waveguide [setup (b) in Fig. 1], if it takes place, is compensated by the radiation absorption in the plasma-waveguide walls. In a slightly divergent conical plasma waveguide, the condition of channeling is easier to satisfy; in this

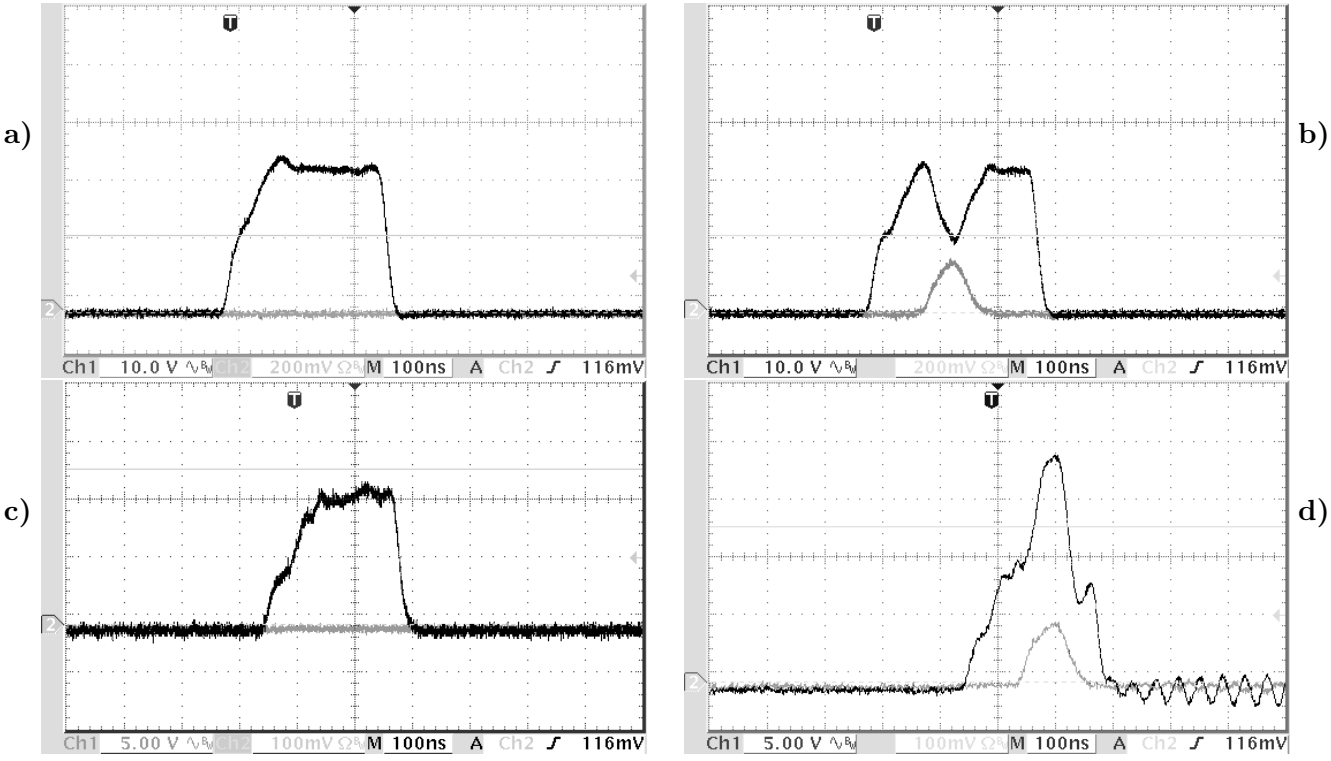

Fig. 3. Signals from the microwave receiver (upper beam) and laser pulse (lower beam): upper (a and b) for the setup in Fig. 1a and lower (c and d) for the setup in Fig. 2d. The distance to the receiver $L = 12$ m.

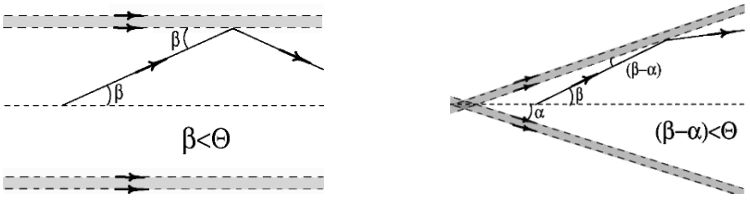

Fig. 4. Schematic view of the microwave-radiation propagation in a cylindrical (left) and conical (right) plasma waveguide.

case, it acquires the form $\beta_{\text{microwave}} - \alpha < \Theta$ (see Fig. 4b). As a consequence, in experiments staged in setups (c) and (d) (Fig. 1) we observe amplification of the microwave signal.

The interaction length of microwave radiation and plasma in a weakly converging waveguide was assessed experimentally by closing the laser beam with a dielectric screen at various distances from the microwave source; the interaction length was found to be about 10 m.

3. Theory of the Sliding-Mode Propagation in Plasma Waveguides

3.1. Dielectric Properties of Weakly Ionized Atmospheric Air Plasma

For theoretical consideration of the realized sliding mode of the microwave radiation propagation in plasma waveguides, we make use of a simplest model.

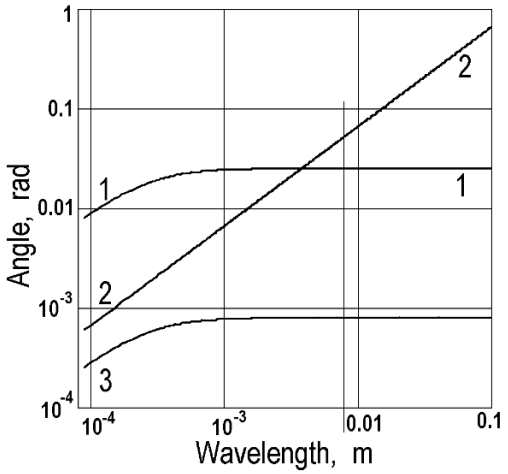

Fig. 5. Diffraction angle and angles of total internal reflection from the plasma–air interface vs the microwave radiation wavelength. Microwave-radiation diffraction angle (1), hydrocarbons added (2), and atmospheric air (3).

We assume a plasma waveguide to be an air cylinder of radius R, bounded by a plasma layer whose thickness significantly exceeds the field-penetration depth. We consider modes of a round waveguide of constant radius $R \gg \lambda$; the density of the plasma is assumed to be homogeneous in cross section and along the propagation length, which is a good approximation under the conditions of our experiment. The diffuse spreading of the waveguide walls is assumed to be small (in comparison with the microwave-signal wavelength) during the pulse action.

The permittivity of a weakly ionized air plasma in the microwave electromagnetic-wave field is approximated by the relation [22]

$$\varepsilon_p = \varepsilon_{\text{air}} - \frac{\Omega_p^2}{\omega(\omega + i\nu_T)}. \tag{1}$$

The permittivity of atmospheric air for the centimeter–submillimeter wavelengths is $\varepsilon_{\text{air}} - 1 \sim 10^{-4}$ [22], so this difference can be neglected, assuming $\varepsilon_{\text{air}} = 1$.

In the experiments under consideration, plasma is formed as a result of direct or stepwise multiphoton ionization of air molecules in the radiation field of a KrF laser ($\lambda_L = 248$ nm and $\hbar\omega_L \approx 5$ eV). The average energy defect in the photoionization of air molecules is ∼1 eV, and, since the electronic component of the plasma is rapidly thermalized (of the order of the electron–electron collision time), it can be assumed that in our problem the characteristic electron temperature T_e is within the range of 0.03–1 eV. An estimate of the effective transfer frequency of collisions of electrons with air molecules at atmospheric pressure is $\nu_T \sim 10^{12}$ s^{-1} [22–24].

With increase in the extent of ionization, the electron–ion collisions begin to play a significant role. The effective frequencies of the electron–electron and electron–ion collisions are assessed by the following relations [22, 25]:

$$\nu_{ee}[\text{s}^{-1}] = \frac{3.7\, n_e[\text{cm}^{-3}]}{T_e^{3/2}[\text{K}]} \ln\Lambda, \qquad \nu_{ei} \approx \frac{\nu_{ee}}{\sqrt{2}}, \tag{2}$$

where the Coulomb logarithm $\ln\Lambda = 7.47 + 3/2 \log T[\text{K}] - 1/2 \log n_e$ [cm^{-3}]. It is easy to see that, under the considered conditions, the electron–ion collisions are insignificant from the viewpoint of the dielectric properties of the plasma within the density range $n_e \le 10^{15} - 10^{16}$ cm^{-3}.

Thus, within the centimeter–submillimeter wavelength range, extended plasma waveguides of the sliding modes in atmospheric air are characterized by the permittivity, for which the following relation of the real and imaginary parts is fulfilled:

$$\text{Re}\,(1 - \varepsilon_p) = \frac{\xi}{1 + \omega^2/nu_T^2} \ll \text{Im}\,(1 - \varepsilon_p) = \frac{\xi}{1 + \omega^2/\nu_T^2} \frac{\nu_T}{\Omega}. \tag{3}$$

Here, $\xi = \Omega_p^2/\nu_T^2 \approx 3.19 \cdot 10^{-3} \cdot \left(ne/10^{12}\ \text{cm}^{-3}\right)$ at the plasma density $n_e \le 10^{15}$ cm^{-3}. This particular feature, as we discussed above, distinguishes plasma waveguides from dielectric waveguides [14, 15].

In the considered waveguides with $R \gg \lambda$, the conditions of internal reflection are, obviously, fulfilled more easily at a smaller characteristic angle of the sliding mode (i.e., the closer the angle of "incidence"

on the waveguide wall to $\pi/2$); due to this fact, we choose as operating modes the lowest axial-symmetric transverse magnetic (TM) (E_{0n}) and transverse electric (TE) (H_{0n}) modes, as well as the EH_{11} mode, which is known to be the main operating mode in dielectric waveguides [14].

3.2. Propagation of Axial-Symmetric Sliding Modes

First, we consider the axial-symmetric modes E_{0n} and H_{0n}.

The transverse distribution of the electromagnetic-field longitudinal components (E_z for TM and H_z for TE modes) has the form $\sim J_0(\varkappa_1 r)\exp[i(hz-\omega t)]$ inside the waveguide and $\sim H_0^{(1)}(\varkappa_2 r)\exp[i(hz-\omega t)]$ in the plasma of the walls, where r and z are the transverse and longitudinal coordinates (the cylindrical coordinate system is used). Correspondingly, the electromagnetic field of the TM mode E_{0n} contains three components (E_z, E_r, H_ϕ), which inside the cylinder (air, $r < R$) have the form [14, 26]

$$E_z = E_0 J_0(\varkappa_1 r), \qquad E_r = -i\frac{h}{\varkappa_1}E_0 J_1(\varkappa_1 r), \qquad H_\phi = -i\frac{k_0}{\varkappa_1}E_0 J_1(\varkappa_1 r) \tag{4}$$

and in ambient plasma, $r > R$,

$$E_z = CH_0^{(1)}(\varkappa_2 r), \qquad E_r = -i\frac{h}{\varkappa_2}CH_1^{(1)}(\varkappa_2 r), \qquad H_\phi = -i\frac{\varepsilon_p k_0}{\varkappa_1}CH_1^{(1)}(\varkappa_2 r). \tag{5}$$

For the orthogonal mode H_{0n}, the field is represented by the components H_z, H_r, E_ϕ and has the form

$$H_z = H_0 J_0(\varkappa_1 r), \qquad H_r = -i\frac{h}{\varkappa_1}H_0 J_1(\varkappa_1 r), \qquad E_\phi = i\frac{k_0}{\varkappa_1}H_0 J_1(\varkappa_1 r) \tag{6}$$

in air and

$$H_z = C'H_0^{(1)}(\varkappa_2 r), \qquad H_r = -i\frac{h}{\varkappa_2}C'H_1^{(1)}(\varkappa_2 r), \qquad E_\phi = i\frac{k_0}{\varkappa_1}C'H_1^{(1)}(\varkappa_2 r) \tag{7}$$

in the plasma. Here, the functions $J_n(x)$ and $H_n^{(1)}(x)$ are Bessel functions and Hankel functions of the first kind, and E_0, C and H_0, C' are the amplitudes of the fields in air and plasma for the TM and TE modes, respectively. The transverse wavenumbers are determined by the dispersion correlations in air and plasma,

$$\varkappa_1^2 = k_0^2 - h^2, \qquad \varkappa_2^2 = \varepsilon_p k_0^2 - h^2, \tag{8}$$

where $k_0 = \omega/c$ is the wavenumber in vacuum.

The boundary conditions (continuity of the tangential components at $r = R$) determine the amplitudes of the field in plasma, $C/E_0 = C'/H_0 = J_0(\varkappa_1 R)/H_0^{(1)}(\varkappa_2 R)$, and the dispersion equation [26]

$$\frac{1}{\varkappa_1 R}\frac{J_1(\varkappa_1 R)}{J_0(\varkappa_1 R)} = \frac{\chi}{\varkappa_2 R}\frac{H_1^{(1)}(\varkappa_2 R)}{H_0^{(1)}(\varkappa_2 R)}, \tag{9}$$

where $\chi = \varepsilon_p$ stands for the TM axial-symmetric modes, and $\chi = 1$ for the TE modes.

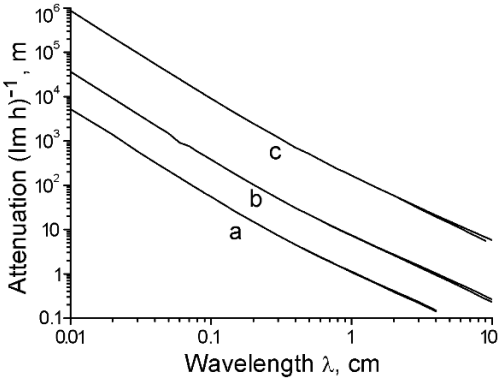

Fig. 6. Dependence of the characteristic attenuation length $(\mathrm{Im}\, h)^{-1}$ of lower axial-symmetric sliding modes of microwave radiation on its wavelength at plasma density $n_e = 10^{12}$ cm^{-3} and waveguide radius $R = 5$ cm (a), 10 cm (b), and 30 cm (c). The lower branches of the curves correspond to E_{01} modes, and the upper branches to H_{01} modes.

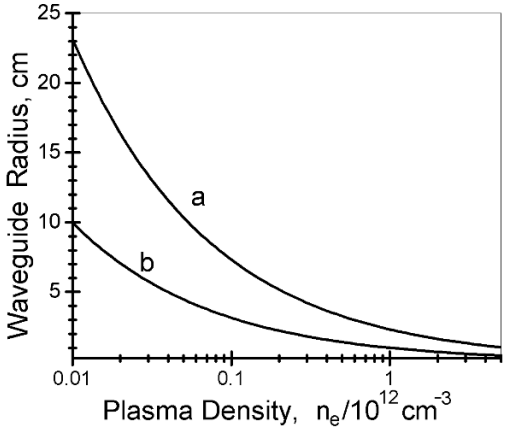

Fig. 7. Characteristic threshold values [relation (10)] of the waveguide radius versus the density of wall plasma for microwave radiation wavelengths $\lambda = 8$ mm (a) and $\lambda = 3$ mm (b).

Since $R/\lambda \gg 1$, dispersion equations (9) have, generally speaking, a number of roots corresponding to various transverse axial-symmetric modes. The greatest propagation length corresponds, apparently, to the minimum value of the transverse wavenumber $\varkappa_1$, i.e., to the lowest transverse mode.

Figure 6 presents the characteristic propagation length $(\mathrm{Im}\, h)^{-1}$ of the sliding axial-symmetric modes (E_{01} and H_{01}) of a plasma waveguide versus the signal wavelength within the centimeter–submillimeter wave range. The calculations were carried out at the plasma density $n_e = 10^{12}$ cm^{-3} for various values of the waveguide radius $R = 5, 10, 30$ cm; the characteristic transfer frequency was taken to be $\nu_T = 10^{12}$ s^{-1}. Under these conditions, $|\varepsilon_p - 1| \ll 1$ and the results for the TE and TM modes practically coincide; some discrepancy begins only at wavelengths $\lambda \geq 1$ cm.

For further analysis, it is convenient to introduce the dimensionless parameter $\mu^2 = \dfrac{(\Omega_p/\nu_T)^2}{1 + (\omega/\nu_T)^2}(k_0 R)^2$. Setting $\varkappa_1 R = x\mu$ and $\varkappa_2 R = y\mu$, we have $x^2 - y^2 = 1 - i\nu_T/\omega$, and the solution of dispersion equation (9) is, in fact, determined by two parameters, μ and ν_T/ω. Numerical analysis makes it possible to determine the threshold value of the parameter μ at which the effective propagation of the sliding mode is possible,

$$\mu_{\mathrm{th}} \approx 1. \tag{10}$$

In the range of parameters $\mu \sim 0.5 - 1$, absorption sharply increases, and at $\mu \leq 0.5$ the propagation almost vanishes — the characteristic propagation length $(\mathrm{Im}\, h)^{-1}$ is limited to several wavelengths. In the domain $\mu > \mu_{\mathrm{th}} = 1$, the propagation regime is stabilized. As $\mu^2 \propto n_e R^2$, relation (10), in fact, determines the lower boundary of plasma densities and waveguide radii at which the sliding propagation regime is realized. In Fig. 7, the indicated boundary of the sliding mode is presented for microwave-signal wavelengths $\lambda = 8$ mm and $\lambda = 3$ mm.

In the limit of large values

$$\mu \gg 1, \qquad \nu_T/\omega \gg 1, \tag{11}$$

for the roots of dispersion equation (9), we succeed in obtaining simple analytical relations, by analogy with those done for large-radius dielectric waveguides [15]. It is easy to see that the root of the dispersion equation occurring near the point $x \approx \alpha/\mu$, where $\alpha \approx 3.83$ is the first root of the Bessel function $J_1(\alpha) = 0$, corresponds to the sliding regime for the lowest axial-symmetric modes E_{01} and H_{01}. For this, it is necessary that

$$|\varepsilon_p| \ll k_0 R\sqrt{\xi\nu_T/\omega}, \tag{12}$$

which indicates the smallness of the coefficient $\chi/\varkappa_2 R \ll 1$ on the right-hand side of (9). Indeed, then $y^2 = i\nu_T/\omega + x^2 - 1$ whence, for the characteristic transverse wavenumber in the plasma of the waveguide wall, we obtain

$$\varkappa_2 = \frac{\mu y}{R} \approx \pm(1+i)\frac{\mu}{R}\sqrt{\frac{\nu_T}{2\omega}}, \tag{13}$$

where the plus sign should be chosen to provide the decay of the field in the plasma with the radius, (5). In accordance with this relation, in the considered limit (11), the argument of the Hankel functions on the right-hand side of dispersion relations (9) is large, $|\varkappa_2 R| \gg 1$, and, making use of the corresponding asymptotic [27], we have $H_1^{(1)}(\mu y)/H_0^{(1)}(\mu y) \approx -i$. The Bessel functions in the neighborhood of the given root $x = \alpha/\mu + \delta x$, $\delta x \ll \alpha/\mu$ are approximated as follows [27]:

$$J_1(\mu x) \approx \mu\delta x\left(1 - \frac{\mu\delta x}{2\alpha}\right)J_0(\alpha), \qquad J_0(\mu x) \approx \left(1 - \frac{1}{2}(\mu\delta x)^2\right)J_0(\alpha) \tag{14}$$

and, since $y \approx (1+i)\sqrt{\frac{\nu_T}{2\omega}}\left(1 - i\frac{\omega}{2\nu_T}\left[\frac{\alpha^2}{\mu^2} - 1\right] - i\frac{\alpha}{\mu}\frac{\omega}{\nu_T}\delta x\right)$, in the lowest order from dispersion equation (9) we obtain

$$\left[1 - 2(1-i)\frac{\alpha\chi}{\mu}\left(\frac{\omega}{2\nu_T}\right)^{3/2}\right]\delta x \approx -(1+i)\frac{\chi\alpha}{\mu^2}\sqrt{\frac{\omega}{2\nu_T}}\left[1 + i\left(\frac{\alpha^2}{\mu^2} - 1\right)\frac{\omega}{2\nu_T}\right]. \tag{15}$$

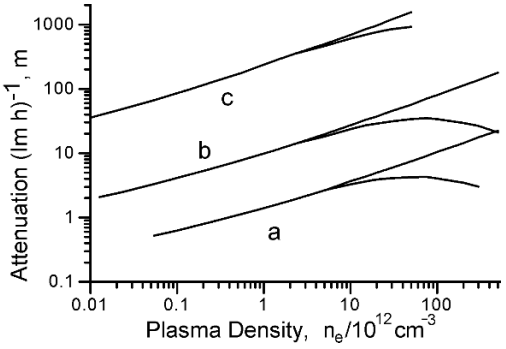

Fig. 8. Dependence of the characteristic attenuation length $(\mathrm{Im}\, h)^{-1}$ of lower axial-symmetric sliding modes of microwave radiation with the wavelength $\lambda = 8$ mm on the density of waveguide wall plasma at waveguide radius $R = 5$ cm (a), 10 cm (b), and 30 cm (c). The lower branches of the curves correspond to E_{01} modes, and the upper branches to H_{01} modes.

Thus, as we demonstrated numerically above (see Fig. 6), for plasma with a low degree of ionization, such that $|\varepsilon_p - 1| \ll 1$ (i.e., $\xi\nu_T/\omega \ll 1$), the solutions for the E_{01} and H_{01} modes practically coincide, and for the attenuation coefficient we have

$$\mathrm{Im}\, h \approx \frac{\alpha^2}{k_0^2 R^3\sqrt{2\xi\nu_T/\omega}}. \tag{16}$$

The characteristic propagation length increases with increase in the frequency of the signal and plasma waveguide radius, $(\mathrm{Im}\, h)^{-1} \propto R^3\omega^{3/2}n_1^{1/2}$. This behavior is supported by numerical investigation of the roots of dispersion equation (9), the results of which are presented in Fig. 8 for the dependence of $(\mathrm{Im}\, h)^{-1}$ on the plasma density within the range of $10^{10} - 10^{14}$ cm^{-3}. The calculations were carried out for the wavelength $\lambda = 8$ mm, corresponding to the experiment, at various values of plasma waveguide radii, $R = 5, 10, 30$ cm.

With increase in the plasma density in the domain $k_0 R \gg \sqrt{\xi\nu_T/\omega} \gg 1$ [in this case, condition (12) is still valid], the solutions for various modes split as shown in Fig. 8. For the mode H_{01}, the root of the dispersion equation remains near $x \sim \alpha/\mu$, and relation (16) is preserved. For the mode E_{01}, the root is gradually shifted with increase in density, $(\mu x - \alpha)/\alpha \propto \sqrt{\xi\nu_T/\omega}/k_0 R$, and for the increment of attenuation of this mode we derive

$$\mathrm{Im}\, h \approx \frac{\alpha^2}{k_0^2 R^3}\sqrt{\frac{\xi\nu_T}{2\omega}}\left(1 + \frac{1}{k_0 R}\sqrt{\frac{\xi\nu_T}{2\omega}}\right), \tag{17}$$

i.e., its characteristic propagation length begins to decrease with density, $\propto n_e^{-1/2}$.

Transition to the regime of a metal waveguide occurs with further density increase and shifts to the domain $\sqrt{\xi\nu_T/\omega} \gg k_0 R$, when relation (12) ceases to be fulfilled. In this regime of high conductance of the walls, the coefficient on the right-hand side of (9) becomes large, $|\xi/\varkappa_2 R| \gg 1$, and, as a consequence, the root of the dispersion equation for the E_{01} mode shifts to the value $\mu x \approx \beta \approx 2.405$ ($J_0(\beta) = 0$), which is characteristic of the E_{01} mode of a metal waveguide. In accordance with the theory of metal waveguides, the increment of attenuation of such a TM mode increases with frequency, $\mathrm{Im}\, h \propto \sqrt{\omega}$, and its minimum value is achieved near the cutoff frequency [14]. In this range of parameters, the optimum propagation conditions are realized at $R \sim \lambda$ [10, 11].

3.3. Propagation of Axial-Asymmetric Sliding Mode $\mathbf{EH}_{11}$

The lowest axial-asymmetric mode EH_{11} is the main operating mode of dielectric waveguides [14]. This is a hybrid mode, i.e., it contains all six components of the electromagnetic field; herewith, all longitudinal components of the electric and magnetic fields have the form $E_z, H_z \sim J_1(\varkappa_1 r)$ inside the waveguide and $E_z, H_z \sim H_1^{(1)}(\varkappa_2 r)$ in plasma of the walls. The dispersion equation for the mode EH_{11} can then be written as [26]

$$\left[\left(\frac{1}{\varkappa_1}\frac{J_0(\varkappa_1 R)}{J_1(\varkappa_1 R)} - \frac{\varepsilon_p}{\varkappa_2}\frac{H_0^{(1)}(\varkappa_2 R)}{J_1(\varkappa_2 R)}\right) - \left(\frac{1}{\varkappa_1^2 R} - \frac{\varepsilon_p}{\varkappa_2^2 R}\right)\right] \times \left[\left(\frac{1}{\varkappa_1}\frac{J_0(\varkappa_1 R)}{J_1(\varkappa_1 R)} - \frac{1}{\varkappa_2}\frac{H_0^{(1)}(\varkappa_2 R)}{J_1(\varkappa_2 R)}\right) - \left(\frac{1}{\varkappa_1^2 R} - \frac{1}{\varkappa_2^2 R}\right)\right] = \left(\frac{1}{\varkappa_1^2 R} - \frac{\varepsilon_p}{\varkappa_2^2 R}\right)\left(\frac{1}{\varkappa_1^2 R} - \frac{1}{\varkappa_2^2 R}\right). \tag{18}$$

By analogy with the case of axial-symmetric modes, this equation can be approximately solved in the limit (11) of large values of the parameter $\mu \gg 1$ and transfer frequency $\nu_T/\omega \gg 1$. It is easy to see that with condition (12) imposed, for plasma with a low extent of ionization $|ve_p - 1| \ll 1$, the root of dispersion equation (18) is near $\mu x \approx \beta \approx 2.405$ ($J_0(\beta) = 0$). Indeed, in this case,

$$\frac{1}{\varkappa_1^2 R} - \frac{\varepsilon_p}{\varkappa_2^2 R} \approx \frac{1}{\varkappa_1^2 R} - \frac{1}{\varkappa_2^2 R}, \tag{19}$$

and Eq. (18) is significantly simplified,

$$\frac{1}{\varkappa_1}\frac{J_0(\varkappa_1 R)}{J_1(\varkappa_1 R)} - i\frac{\varepsilon_p}{\varkappa_2} \approx \frac{1}{\varkappa_1}\frac{J_0(\varkappa_1 R)}{J_1(\varkappa_1 R)} - \frac{i}{\varkappa_2} \approx 0. \tag{20}$$

Here we made use of the asymptotics of the Hankel functions $H_0^{(1)}(\mu y)/H_1^{(1)}(\mu y) \approx i$ at large values of the argument $\mu y \gg 1$. Decomposing the dispersion equation in the neighborhood of this root $x = \beta/\mu + \delta x$, $\delta x \ll \beta/\mu$, we obtain $J_0(\mu x) \approx -J_1(\beta)\mu\,\delta x$, and for the approximate value of the root (20) we have

$$\delta x \approx -(1+i)\frac{\beta}{\mu^2}\sqrt{\frac{\omega}{2\nu_T}}. \tag{21}$$

As a result, for the increment of attenuation of the EH_{11} mode, we obtain the relation

$$\mathrm{Im}h \approx \frac{\beta^2}{k_0^2 R^3\sqrt{2\xi\nu_T/\omega}}, \tag{22}$$

similar to (16). Thus, the characteristic propagation length of the hybrid mode EH_{11} exceeds the propagation length of the axial-symmetric mode $(\alpha/\beta)^2 \approx 2.54$ times.

At the densities $k_0 R \gg \sqrt{\xi\nu_T/\omega} \gg 1$, we arrive, similarly to (17), at the estimate

$$\operatorname{Im} h \approx \frac{\beta^2}{k_0^2 R^3}\sqrt{\frac{\xi\nu_T}{2\omega}}\,. \tag{23}$$

This result is supported by the numerical solution of dispersion equation (18) under the condition of realizing the sliding regime. Figure 9 presents the dependences of the characteristic propagation length $(\operatorname{Im} h)^{-1}$ of the hybrid mode EH_{11} of a plasma waveguide on the wavelength of the centimeter–submillimeter wave signal, for parameters corresponding to Fig. 3 for the case of axial-symmetric modes. Figure 10 presents the dependences of $(\operatorname{Im} h)^{-1}$ on the plasma density for the corresponding wavelength $\lambda = 8$ mm at various values of the plasma waveguide radius, $R = 5, 10, 30$ cm.

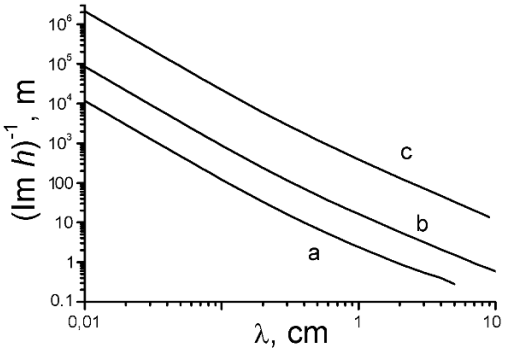

Fig. 9. Dependence of the characteristic attenuation length $(\operatorname{Im} h)^{-1}$ of the lower hybrid mode EH_{11} of microwave radiation on its wavelength at plasma density $n_e = 10^{12}$ cm^{-3} and waveguide radius $R = 5$ cm (a), 10 cm (b), and 30 cm (c).

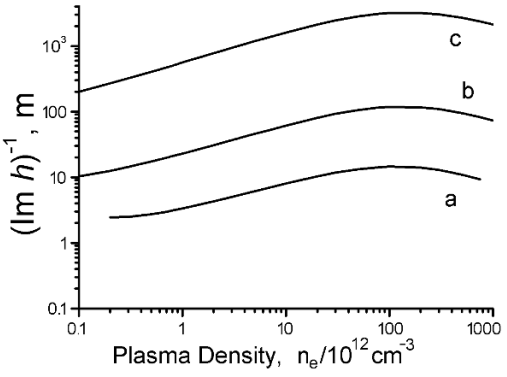

Fig. 10. Dependence of the characteristic attenuation length $(\operatorname{Im} h)^{-1}$ of the lower hybrid mode EH_{11} of microwave radiation with the wavelength $\lambda = 8$ mm on the density of waveguide wall plasma at waveguide radius $R = 5$ cm (a), 10 cm (b), and 30 cm (c).

3.4. Effect of the Thickness of Plasma Waveguide Walls

The previous consideration was carried out in the limit of infinitely thick walls of plasma waveguides, such that the wave practically does not escape to the external space — the characteristic depth of field-into-plasma penetration is small in comparison with the wall thickness d, $\varkappa_2 d = \mu y d/R \gg 1$. Nevertheless, the wall thickness apparently significantly affects the characteristic length of the sliding mode propagation — the losses increase in thin walls due to "outflow" (re-emission) of the sliding modes "sideways." At the same time, an increase in the thickness of the plasma walls of extended waveguides implies, in fact, a significant increase in the energy consumption of the ionizing laser pulse.

Thus, from the viewpoint of optimizing the geometry of the transfer, of interest is the study of the dependence of the attenuation length of the sliding mode of microwave radiation on the thickness of plasma waveguide walls. In this work, we restrict ourselves to the case of the axial-symmetric mode E_{01}.

We consider the plasma waveguide to be a cylinder; the radius of the internal wall of the waveguide is R_1, and that of the external wall R_2. The field structure of the E_{01} mode in the internal field of the

waveguide, $r < R$, is determined by expressions (4), and in the region occupied by plasma, $R_1 < r < R_2$, we have

$$\begin{aligned} E_z &= AJ_0(\varkappa_2 r) + BH_0^{(1)}(\varkappa_2 r), \\ E_r &= -\frac{ih}{\varkappa_2}\left[AJ_1(\varkappa_2 r) + BH_1^{(1)}(\varkappa_2 r)\right], \\ H_\phi &= -\frac{i\varepsilon_p k_0^2}{\omega\varkappa_2}\left[AJ_1(\varkappa_2 r) + BH_1^{(1)}(\varkappa_2 r)\right] \end{aligned} \tag{24}$$

and

$$E_z = CH_0^{(1)}(\varkappa_1 r), \qquad E_r = -C\frac{ih}{\varkappa_1}H_1^{(1)}(\varkappa_1 r), \qquad H_\phi = -C\frac{ik_0^2}{\omega\varkappa_1}H_1^{(1)}(\varkappa_1 r) \tag{25}$$

in the ambient space, $r > R_2$. Herewith, for the transverse wavenumbers, relations (18) are preserved.

Making use of the boundary conditions, i.e., the continuity of the tangential components of the field at $r = R_1$ and $r = R_2$, we obtain for the amplitudes of the field components in plasma

$$\begin{aligned} A &= E_0\frac{J_0(\varkappa_1 R_1)H_1^{(1)}(\varkappa_2 R_1) - [\varkappa_2/(\varepsilon_p\varkappa_1)]J_1(\varkappa_1 R_1)H_0^{(1)}(\varkappa_2 R_1)}{J_0(\varkappa_2 R_1)H_1^{(1)}(\varkappa_2 R_1) - J_1(\varkappa_2 R_1)H_0^{(1)}(\varkappa_2 R_1)} \\ &= C\frac{H_0^{(1)}(\varkappa_1 R_2)H_1^{(1)}(\varkappa_2 R_2) - [\varkappa_2/(\varepsilon_p\varkappa_1)]H_1^{(1)}(\varkappa_1 R_2)H_0^{(1)}(\varkappa_2 R_2)}{J_0(\varkappa_2 R_2)H_1^{(1)}(\varkappa_2 R_2) - J_1(\varkappa_2 R_2)H_0^{(1)}(\varkappa_2 R_2)}, \\ B &= -E_0\frac{J_0(\varkappa_1 R_1)J_1(\varkappa_2 R_1) - [\varkappa_2/(\varepsilon_p\varkappa_1)]J_1(\varkappa_1 R_1)J_0(\varkappa_2 R_1)}{J_0(\varkappa_2 R_1)H_1^{(1)}(\varkappa_2 R_1) - J_1(\varkappa_2 R_1)H_0^{(1)}(\varkappa_2 R_1)} \\ &= -C\frac{H_0^{(1)}(\varkappa_1 R_2)J_1(\varkappa_2 R_2) - [\varkappa_2/(\varepsilon_p\varkappa_1)]H_1^{(1)}(\varkappa_1 R_2)J_0(\varkappa_2 R_2)}{J_0(\varkappa_2 R_2)H_1^{(1)}(\varkappa_2 R_2) - J_1(\varkappa_2 R_2)H_0^{(1)}(\varkappa_2 R_2)}. \end{aligned} \tag{26}$$

Finally, the dispersion equation is obtained in the form

$$\begin{aligned} \frac{J_1(\varkappa_1 R_1)}{J_0(\varkappa_1 R_1)} - \frac{\varepsilon_p\varkappa_1}{\varkappa_2}\frac{H_1^{(1)}(\varkappa_2 R_1)}{H_0^{(1)}(\varkappa_2 R_1)} &= \frac{H_0^{(1)}(\varkappa_2 R_2)J_0(\varkappa_2 R_1)}{H_0^{(1)}(\varkappa_2 R_1)J_0(\varkappa_2 R_2)}\left[\frac{J_1(\varkappa_1 R_1)}{J_0(\varkappa_1 R_1)} - \frac{\varepsilon_p\varkappa_1}{\varkappa_2}\frac{J_1(\varkappa_2 R_1)}{J_0(\varkappa_2 R_1)}\right] \\ &\times\left\{\frac{H_1^{(1)}(\varkappa_1 R_2)}{H_0^{(1)}(\varkappa_1 R_2)} - \frac{\varepsilon_p\varkappa_1}{\varkappa_2}\frac{H_1^{(1)}(\varkappa_2 R_2)}{H_0^{(1)}(\varkappa_2 R_2)}\right\}\left\{\frac{H_1^{(1)}(\varkappa_1 R_2)}{H_0^{(1)}(\varkappa_1 R_2)} - \frac{\varepsilon_p\varkappa_1}{\varkappa_2}\frac{J_1(\varkappa_2 R_2)}{J_0(\varkappa_2 R_2)}\right\}^{-1}. \end{aligned} \tag{27}$$

The left-hand side of the dispersion equation coincides with dispersion equation (9) for the sliding axial-symmetric TM mode in the limit of a thick waveguide wall.

The effect of the finite wall thickness is taken into account on the right-hand side. This effect can be understood qualitatively by making use of the following considerations. At sufficiently large $\mathrm{Re}\, z$ and $\mathrm{Im}\, z$, the ratio $H_1^{(1)}(z)/H_0^{(1)}(z) \to -i$, and the right-hand side of the dispersion equation is determined mainly by the first multiplier. Due to the asymptotic behavior of the Hankel functions [27],

$$\frac{H_0^{(1)}(\varkappa_2 R_2)}{H_0^{(1)}(\varkappa_2 R_1)} \sim \exp[-\mathrm{Im}\,\varkappa_2(R_2 - R_1)]. \tag{28}$$

Thus, with increase in the waveguide wall thickness, the effect of the second boundary decreases exponentially. The result of numerical analysis of the dispersion equation is shown in Fig. 11, where the dependence of the attenuation length of the sliding mode on the wall thickness of the plasma waveguide for values of parameters close to the experimental values is presented. The calculations were performed at wavelength $\lambda = 8$ mm for the case of plasma density $n_e = 10^{13}$ cm^{-1} and waveguide internal radius $R_1 = 10$ cm. The curves correspond to the characteristic transfer frequency of collisions $\nu_T = 10^{12}$ cm^{-1}; herewith, the parameter $\mu \approx 13.86$. The calculations show that the effect of the external boundary of the plasma waveguide is insignificant up to a relative wall thickness of ∼10%, i.e., ∼1 cm for the given parameters. The local maxima on the curves are, obviously, of an interference character.

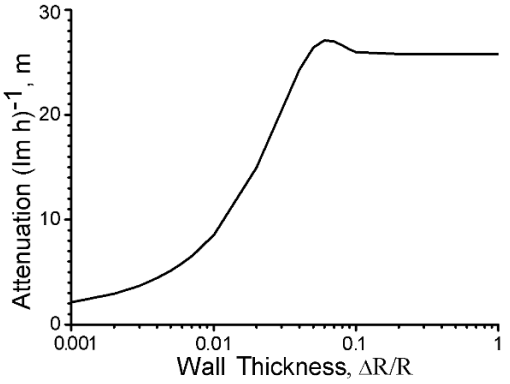

Fig. 11. Dependence of the characteristic attenuation length $(\mathrm{Im}\, h)^{-1}$ of the axial-symmetric mode E_{01} of microwave radiation with wavelength $\lambda = 8$ mm on the relative plasma-waveguide-wall thickness $\Delta R/R$. The result of numerical solutions of dispersion equation (27) at plasma density $n_e = 10^{13}$ cm^{-3} and waveguide radius $R = 10$ cm.

4. Conclusions

To conclude, in this paper we presented the results of a theoretical and experimental study of the sliding mode of the microwave radiation transfer in plasma waveguides in atmospheric air. The mechanism of the transfer is based on the effect of total reflection at the interface with an optically less dense medium and does not require high conductance (density) of plasma. The transfer of a microwave signal, $\lambda = 8$ mm, to a distance over 60 m was experimentally demonstrated. The results of calculations are in good agreement with the experiment and convincingly demonstrate the advantage of the sliding-mode propagation in comparison with high-density plasma waveguides — the power inputs for a waveguide to be developed prove to be lower, and the range of microwave-radiation directed transfer increases with decrease in wavelength and reaches several kilometers for submillimeter waves.

Acknowledgments

This work is dedicated to the memory of Prof. A. G. Molchanov, numerous discussions with whom stimulated its staging. The authors are also grateful to Dr. L. L. Losev and Dr. V. I. Shvedunov for useful discussions and assistance in setting up the experiments. The work was supported by the Educational Scientific Complex of the P. N. Lebedev Physical Institute and the Russian Foundation for Basic Research under Project No 09-07-13593.

References

1. A. N. Kondratenko, *Plasma Waveguides* [in Russian], Atomizdat, Moscow (1976).
2. G. A. Askar'yan, M. S. Rabinovich, M. M. Savchenko, and A. D. Smirnova, *Pisma ZhÉTF*, **1**, 18 (1965).
3. G. A. Askar'yan, *Zh. Éksp. Teor. Fiz.*, **55**, 1400 (1968).

4. G. A. Askaryan and I. M. Rayevsky, *Pisma ZhTF*, **8**, 1131 (1982).
5. V. I. Kolpakov, L. V. Norinsky, and V. S. Rogov, *Pisma ZhTF*, **17**, 67 (1991).
6. V. I. Kolpakov and L. V. Norinsky, *Pisma ZhTF*, **18 (12)**, 55 (1992).
7. A. Braun, G. Korn, X. Liu, et al., *Opt. Lett.*, **20**, 73 (1995).
8. E. T. J. Nibbering, P. F. Curley, G. Grillon, et al., *Opt. Lett.*, **21**, 62 (1996).
9. A. Brodeur, C. Y. Chien, F. A. Ilkov, et al., *Opt. Lett.*, **22**, 304 (1997).
10. A. E. Dormidondov, V. V. Valuev, V. L. Dmitriev, et al., *Proc. SPIE*, **6733**, 67332S (2007).
11. M. Chateauneuf, S. Payeur, J. Dubois, and J.-C. Kieffer, *Appl. Phys. Lett.*, **92**, 091104 (2008).
12. R. R. Musin, M. N. Schneider, A. M. Zheltikov, and R. B. Miles, *Appl. Opt.*, **46**, 5593 (2007).
13. L. L. Losev, "Parametric transformation of the laser radiation in combined active media and in optical breakdown plasma" [in Russian], PhD Thesis, P. N. Lebedev Physical Institute, Moscow (2003).
14. L. A. Vainshtein, *Electromagnetic Waves* [in Russian], Radio i Svyaz, Moscow (1988).
15. B. Cros, C. Courtois, G. Matthieussent, et al., *Phys. Rev. E*, **65**, 026405 (2002).
16. F. Dorchies, J. R. Marques, B. Cros, et al., *Phys. Rev. Lett.*, **82**, 4655 (1999).
17. S. Jackel, R. Burris, J. Grun, et al., *Opt. Lett.*, **20**, 1086 (1995).
18. M. Borghesi, A. J. Mackinnon, R. Gaillard, et al., *Phys. Rev. E*, **57**, R4899 (1988).
19. V. D. Zvorykin, A. O. Levchenko, A. G. Molchanov, et al., *Kr. Soobshch. Fiz. FIAN*, No. 3 (2010).
20. V. D. Zvorykin, A. O. Levchenko, I. V. Smetanin, and N. N. Ustinovsky, *Pisma ZhÉTF*, **91**, 244 (2010).
21. N. G. Basov, A. D. Vadkovsky, V. D. Zvorykin, et al., *Kvantovaya Élektron.*, **21**, 15 (1994).
22. Yu. P. Raizer, *Gas Discharge Physics* [in Russia], Nauka, Moscow (1987) [English translation: Springer, Berlin (1991)].
23. A. G. Engelhardt, A. V. Phelps, and C. G. Risk, *Phys. Rev. A*, **135**, 1556 (1964).
24. O. A. Gordeyev, A. P. Kalinin, A. L. Komov, et al., *Reviews on the Thermophysical Properties of Substances* [in Russian], Institute of High Temperatures of the Russian Academy of Sciences, Moscow (1985), Vol. 5, iss. 55.
25. L. Spitzer, *Physics of Ionized Gases*, Wiley, New York, London (1962).
26. J. A. Stratton, *Electromagnetic Theory*, McGraw-Hill, London (1941).
27. M. Abramowitz and I. A. Stegun, *Handbook of Mathematical Functions*, National Bureau of Standards (1964).